International Journal of Solids and Structures 46 (2009) 3290–3300

Contents lists available at ScienceDirect

International Journal of Solids and Structures

journal homepage: www.elsevier.com/locate/ijsolstr

Wave propagation in a sandwich structure

Liping Liu [a,*], Kaushik Bhattacharya [b]

[a] Department of Mechanical Engineering, University of Houston, Houston, TX 77204-4006, USA
[b] Division of Engineering and Applied Science, Mail Stop 104-44, California Institute of Technology, Pasadena, CA 91125, USA

ARTICLE INFO

Article history:
Received 5 January 2008
Received in revised form 31 March 2009
Available online 6 May 2009

Keywords:
Wave propagation
Transfer matrix
Sandwich structure
Mindlin plate theory

ABSTRACT

The propagation of elastic waves in a sandwich structure with two thin stiff face-plates and a thick compliant core is considered in this paper. A complete description of the dispersion relation with no restrictions on frequency and wavelength is provided. This is accomplished by transforming the wave equation to a Hamiltonian system and then using a transfer matrix approach for solving the Hamiltonian system. To provide insight, particular regimes of the frequency–wavelength plane are then considered. First, an explicit formula is derived for all natural frequencies at the long wavelength limit. It is shown that all waves with finite limiting frequency have zero group velocity, while those with vanishing limiting frequency correspond to longitudinal, shear and flexural waves. The displacement of the flexural waves are reminiscent of Mindlin plates, and an asymptotic procedure to find the shear correction factor is presented. Second, the lowest branch of the dispersion relation is studied in detail and mode shapes are used to motivate explicit but accurate description of this lowest branch. This approximate model is anticipated to be useful in simulations of large structures with sandwich structures.

1. Introduction

Sandwich structures are widely used in diverse applications such as spacecraft, aircraft, automobiles, boats and ships due to their substantial bending strength and impact resistance at a light weight (see for example Thomsen et al. (2005) and the references there). The dynamic applications have motivated various studies of wave propagation and dynamic flexural deformation of multilayer beams and plates. It has long been recognized that shear and internal modes play a critical role in determining the transmission of waves. Consequently, an essential question has been to find an adequate description of such structures that has enough detail to capture the required mechanics but simple enough to be used in engineering computations of large structures. The use of Timoshenko beam and Mindlin plate models that incorporate shear degrees of freedom is common, but also found inadequate for some purposes. Therefore this remains an active area of research.

A common approach is to introduce higher order models by making various kinematic ansatz. Mead and Markus (1969) introduced a sixth-order model that neglects rotational inertia. Frostig and Baruch (1994) developed a general approach for systematically deriving higher order models starting from Hamilton's principles. Yang and Qiao (2005) recently followed this approach to develop a numerical approach for beams. Backström and Nilsson (2006) start with a sixth order theory and use it to fit a fourth-order model with frequency-dependent coefficients, and showed that these match well with experiments (Backström and Nilsson, 2007). An interesting variation is the recent work of Bonfiglioa et al. (2007) who used a spectral finite element method which enables them to capture some internal modes. In any case, all these works are based on significant *a priori* ansatz about the deformation.

The works of Nilsson (1990), Nosier et al. (1993) and Sorokin (2004, 2006) study the problem more generally by considering field equations and using it to understand all possible waves in a sandwich structure. Nilsson (1990) and Sorokin (2004) treat the face-plates as plates and use a fourth-order theory to describe the lateral displacements while retaining the full elastic equations of the core. Nosier et al. (1993) study the deformation of the various layers and then couple them all together using a transfer matrix. Sorokin (2006) concentrates on pure shear deformations of a sandwich plate. Our work continues this line of thinking.

We consider an infinite sandwich structure and describe a general method to compute the dispersion relations of all propagating waves. This provides a benchmark for the accuracy of various approximate models described above. Specifically, we consider the field equations of elasticity for the entire structure with appropriate interfacial jump conditions with no a priori assumptions. We show that we can rewrite these governing equations as a Hamiltonian system following Atkinson (1964), and solve the Hamiltonian system using the method of *transfer matrix* (Haskell, 1953; Knopoff, 1964). We use particular properties of the Hamiltonian system to characterize the dispersion relation and compute it for a specific example.

* Corresponding author. Tel.: +1 6263954125; fax: +1 6317911034.
E-mail addresses: liuliping@uh.edu (L. Liu), bhatta@caltech.edu (K. Bhattacharya).

0020-7683/$ - see front matter © 2009 Elsevier Ltd. All rights reserved.
doi:10.1016/j.ijsolstr.2009.04.023

While the method described above is rigorous and complete, it is somewhat obscure. It does not provide any explicit formulas, and the dispersion equation provides little information about the mode shapes. We therefore elaborate on two regimes of interest. We do so for a specific example, but note that the methods are broadly applicable and the results representative.

We first focus on the long wavelength regime. We provide an explicit formula for all natural frequencies in the long wavelength limit, in-plane wave-vector $\mathbf{k} \to 0$. We are able to do so by exploiting the fact that the relevant block of the transfer matrix becomes diagonal in this limit. To our knowledge, such an explicit formula is new for heterogeneous laminated structures.

It is in fact possible to obtain further information by perturbatively studying the dispersion relation $\omega_\alpha(\mathbf{k})$ around $\mathbf{k} = 0$. We note that the global transfer matrix associated with the structure is an analytic matrix-valued function of $\mathbf{k}$, and hence it can be expressed as a power series in $\mathbf{k}$. If this series is truncated up to certain finite order, we obtain an algebraic equation that determines the coefficients of the Taylor expansion of $\omega_\alpha(\mathbf{k})$ up to the same order. The explicit implementation of this method is hindered by the complicated algebra, but nevertheless provides interesting insights. It can be used to show that the group velocity of every wave with a non-zero limiting frequency is zero. Further there are exactly three branches for which the frequency tends to zero with wave number, corresponding to the longitudinal, shear and flexural waves. Finally, we seek to investigate the lowest of these branches, the flexural branch. While the algebra becomes too involved for a heterogeneous plate, we show that it recovers the well-known formula $D_0 = E_0 h^3/12(1-\nu_0^2)$ for the flexural rigidity of an isotropic homogeneous plate of Young's modulus E_0 and Poisson's ratio ν_0. We also argue that such a procedure applied to a heterogeneous plate is in fact the natural way to determine the correction factor on the transverse shear modulus of the Mindlin plate theory (Mindlin, 1951; Stephen, 1997).

This brings us to the second regime of interest, the lowest branch of the dispersion relation. We describe the mode shapes for various wavelengths. At long wavelengths, the waves are flexural. We show that approximating the sandwich structure using the Mindlin plate theory (also referred to as Timoshenko–Mindlin plate theory or Reissner–Mindlin plate theory in the literature, see Timoshenko, 1921, 1922, Reissner, 1945, 1947 and Mindlin, 1951) describes the dispersion relation well for long and intermediate wavelengths up to a thickness of wavelength ratio of 0.8. The simpler Kirchhoff–Love theory provides agreement only in a very limited range of very long wavelengths with significant deviations at a thickness of wavelength ratio of 0.02. The difference between these theories is the inclusion of transverse shear, and this is significant in a sandwich structure with stiff face-plates and compliant core.

At shorter wavelengths, the waves change to a coupled mode involving flexure of the face-plates and dilatation of the core. We develop a simplified theory for this regime where we use the Kirchhoff–Love plate theory for the face-plates, elasticity neglecting the in-plane shear for the core. We show that the dispersion relation of this theory agrees well not only at intermediate wavelengths as expected, but also surprisingly over the entire range of wavelengths under consideration. Further, the mode shapes of this approximate theory approaches the mode shapes of the Mindlin plate for long wavelengths.

Finally, at very short wavelengths, we find that the lowest branch corresponds to the propagation of shear waves in the core. However, other modes have similar dispersion: indeed, relative difference between the lowest four branches is less than 3%. Thus, in this range the entire dynamics of the sandwich structure become important.

In this study we do not address the transient problem, and so we ignore non-propagating (evanescent) waves and dissipation. These could be accounted in our framework of transfer matrix by allowing the wavevector to be complex for evanescent waves, and the frequency and elasticity tensor to be complex for dissipation. However, there are mathematical difficulties. Specifically, the validity of Theorem 1 is not clear and thus it is not clear if a solution exists for the governing wave equations (2). Further, there may be instabilities in the numerical solution of the equations, see Castaings and Hosten (1994).

The new features of our work are as follows. We develop a new approach for studying all waves in a multilayer structure. Specifically, we start with the equations of elastodynamics in every layer including the face-plates. We rewrite the governing equations as a Hamiltonian system and this allows us to the transfer matrix associated with each layer as the exponential of the corresponding Hamiltonian (matrix). Further, the convenient properties of the transfer matrix become self-evident from the definition of a Hamiltonian matrix (cf., Nayfeh, 1995, Chapter 9). We provide detailed description of waves in a sandwich structure and explore various regimes. In the long wavelength limit, we derive an explicit formula for computing all the natural frequencies of a sandwich structure. Further, the transfer matrix formulation provides a systematic way to expand and truncate the dispersion equation in power series of the wavenumber $|\mathbf{k}|$, which enables us to justify various models by comparing the dispersion equations of the approximate models with the truncated dispersion equations of the exact theory. Finally, we explain the mysterious "correction factor" in the Mindlin plate theory: it arises from the inconsistence between the kinematic hypothesis and the desired accuracy of the Mindlin plate theory.

The paper is organized as follows. In Section 2, we present the exact formal solution of the wave equation for the sandwich structure based on the transfer matrix method. We numerically calculate the full spectrum for a particular sandwich structure. In Section 3, we present the formulas for the natural frequencies $\omega_\alpha(0)$ at zero wave number and the perturbation method for calculating the correction terms of the dispersion relations $\omega_\alpha(\mathbf{k})$ around $\mathbf{k} = 0$. In Section 4, we focus on the lowest branch of the dispersion relations, for which three simplified models are found useful. We summarize our results in Section 5.

2. The spectrum of a sandwich structure

Let $\{\mathbf{e}_1, \mathbf{e}_2, \mathbf{e}_3\} \subset IR^3$ be the basis for our rectangular coordinate system. Consider an infinite sandwich structure $\Omega_h = \{\mathbf{x} \in IR^3 : 0 < x_3 < h\}$ as shown in Fig. 1. Denote by h_1, h_2, h_3, and h the thickness of the bottom, middle, top layer, and the total thickness of the sandwich structure respectively. Clearly, $h = h_1 + h_2 + h_3$. The elasticity tensor $\mathbf{L}(\mathbf{x})$ and density $\rho(\mathbf{x})$ are given by

$$\mathbf{L}(\mathbf{x}) = \begin{cases} \mathbf{L}_3 & \text{if } h_1+h_2 < x_3 < h \\ \mathbf{L}_2 & \text{if } h_1 < x_3 < h_1+h_2 \\ \mathbf{L}_1 & \text{if } 0 < x_3 < h_1 \end{cases} \text{ and } \rho(\mathbf{x}) = \begin{cases} \rho_3 & \text{if } h_1+h_2 < x_3 < h, \\ \rho_2 & \text{if } h_1 < x_3 < h_1+h_2, \\ \rho_1 & \text{if } 0 < x_3 < h_1. \end{cases} \tag{1}$$

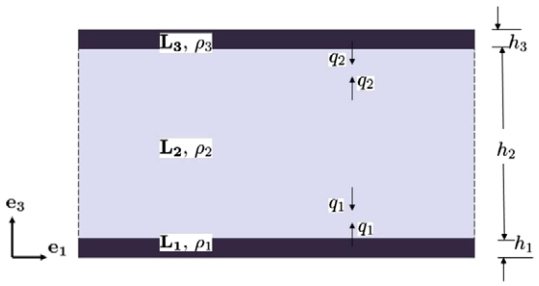

Fig. 1. A typical sandwich structure.

To study the dynamic behavior of this sandwich structure, we consider the following system of partial differential equations for $\mathbf{u}:\Omega_h\times[0,+\infty)\to\mathbb{C}^3$:

$$\begin{cases}\operatorname{div}[\mathbf{L}(\mathbf{x})\nabla\mathbf{u}(\mathbf{x},t)]=\rho(\mathbf{x})\frac{\partial^2}{\partial t^2}\mathbf{u}(\mathbf{x},t) & \forall\mathbf{x}\in\Omega_h,\\ [\mathbf{L}(\mathbf{x})\nabla\mathbf{u}(\mathbf{x},t)]\mathbf{e}_3=0 & \forall\mathbf{x}\in\Gamma_0\cup\Gamma_h,\end{cases}\tag{2}$$

where $\Gamma_{x_3^0}=\{\mathbf{x}:x_3=x_3^0\}$ denote the plane with normal $\mathbf{e}_3$.

We observe that Eq. (2) is invariant under all translations in the plane Γ_0. To describe the long-time response, we restrict ourselves to solutions of form

$$\mathbf{u}(\mathbf{x},t)=\hat{\mathbf{u}}(x_3)\exp(i\mathbf{k}\cdot\mathbf{x})\exp(i\omega t),\tag{3}$$

where $\omega>0$ is the frequency and $\mathbf{k}\in\Gamma_0$ is an in-plane wavevector. Notice that this form ignores evanescent waves and dissipation unless $\mathbf{k},\omega,\mathbf{L}$ are treated as complex. Substituting Eq. (3) into Eq. (2) we obtain

$$\mathbf{T}(x_3)\hat{\mathbf{u}}''(x_3)+i|\mathbf{k}|(\mathbf{R}(x_3)+\mathbf{R}(x_3)^T)\hat{\mathbf{u}}'(x_3)-(|\mathbf{k}|^2\mathbf{Q}(x_3)-\rho\omega^2\mathbf{Id}_3)\hat{\mathbf{u}}(x_3)=0\tag{4}$$

for all $x_3\in(0,h_1)\cup(h_1,h_1+h_2)\cup(h_1+h_2,h)$, where $(')$ denotes d/dx_3, $\mathbf{Id}_m$ is the $m\times m$ identity matrix, and the matrices $\mathbf{Q},\mathbf{R},\mathbf{T}$ are given by ($\hat{\mathbf{k}}=\mathbf{k}/|\mathbf{k}|$)

$$\mathbf{Q})_{pq}=(\mathbf{L})_{piqj}(\hat{\mathbf{k}})_i(\hat{\mathbf{k}})_j,\ \ (\mathbf{R})_{pq}=(\mathbf{L})_{piqj}(\hat{\mathbf{k}})_i(\mathbf{e}_3)_j,(\mathbf{T})_{pq}=(\mathbf{L})_{piqj}(\mathbf{e}_3)_i(\mathbf{e}_3)_j.\tag{5}$$

Note that the matrices $\mathbf{Q},\mathbf{R},\mathbf{T}$ in Eq. (5) depend on x_3 and $\mathbf{k}$, though this is suppressed in the notation for simplicity. Further, the surface traction on $\Gamma_{x_3^0}=\{x:x_3=x_3^0\}$ is expressed as

$$[\mathbf{L}(x_3^0)\nabla\mathbf{u}(\mathbf{x},t)]\mathbf{e}_3=[\mathbf{T}\hat{\mathbf{u}}'(x_3^0)+i|\mathbf{k}|\mathbf{R}^T\hat{\mathbf{u}}(x_3^0)]\exp(i\mathbf{k}\cdot\mathbf{x})\exp(i\omega t).\tag{6}$$

Finally we require that

$$\hat{\mathbf{u}}(x_3)\text{ and }\mathbf{T}\hat{\mathbf{u}}'(x_3)+i|\mathbf{k}|\mathbf{R}^T\hat{\mathbf{u}}(x_3)\text{ are continuous for all }x_3\in(0,h).\tag{7}$$

We now rewrite this as a Hamiltonian system. Let

$$\phi=\begin{bmatrix}\hat{\mathbf{u}}\\ \mathbf{T}\hat{\mathbf{u}}'+i|\mathbf{k}|\mathbf{R}^T\hat{\mathbf{u}}\end{bmatrix}.\tag{8}$$

In terms of ϕ, Eq. (4) can be equivalently written as

$$\phi'(x_3)=\mathbf{H}(\omega,\mathbf{k})\phi(x_3)\quad\forall x_3\in(0,h_1)\cup(h_1,h_1+h_2)\cup(h_1+h_2,h),\tag{9}$$

where

$$\mathbf{H}(\omega,\mathbf{k})=\begin{bmatrix}-i|\mathbf{k}|\mathbf{T}^{-1}\mathbf{R}^T & \mathbf{T}^{-1}\\ |\mathbf{k}|^2(\mathbf{Q}-\mathbf{R}\mathbf{T}^{-1}\mathbf{R}^T)-\rho\omega^2\mathbf{Id}_3 & -i|\mathbf{k}|\mathbf{R}\mathbf{T}^{-1}\end{bmatrix}.\tag{10}$$

The matrix $\mathbf{H}$ is a *Hamiltonian* in the sense that $\mathbf{J}^{-1}\mathbf{H}\mathbf{J}=-\mathbf{H}^*$, where $(*)$ denotes the conjugate transpose (hermitian) and

$$\mathbf{J}=\begin{bmatrix}0 & -\mathbf{Id}_3\\ \mathbf{Id}_3 & 0\end{bmatrix}.\tag{11}$$

Clearly $-\mathbf{J}=\mathbf{J}^{-1}$ and $(\mathbf{J}\mathbf{H})^*=\mathbf{J}\mathbf{H}$. In the literature, Eq. (9) is referred to as a *Hamiltonian system* and often written as

$$\mathbf{J}\phi'(x_3)=(\omega^2\mathbf{A}+\mathbf{B}(\mathbf{k}))\phi(x_3)\ \ \forall x_3\in(0,h_1)\cup(h_1,h_1+h_2)\cup(h_1+h_2,h),\tag{12}$$

where

$$\mathbf{A}=\begin{bmatrix}\rho\mathbf{Id}_3 & 0\\ 0 & 0\end{bmatrix}\quad\text{and}\quad\mathbf{B}(\mathbf{k})=\begin{bmatrix}-|\mathbf{k}|^2(\mathbf{Q}-\mathbf{R}\mathbf{T}^{-1}\mathbf{R}^T) & i|\mathbf{k}|\mathbf{R}\mathbf{T}^{-1}\\ -i|\mathbf{k}|\mathbf{T}^{-1}\mathbf{R}^T & \mathbf{T}^{-1}\end{bmatrix}$$

are two hermitian matrices. In terms of $\phi:(0,h)\to\mathbb{C}^6$, the boundary conditions in Eq. (2) and the requirement of Eq. (7) can be restated as that for some $\xi\in\mathbb{C}^6$, we have

$$\phi(0)=\mathbf{M}\xi,\ \ \phi(h)=\mathbf{N}\xi\quad\text{and}\quad\phi(x_3)\text{ is continuous on }(0,h),\tag{13}$$

where the 6×6 matrices $\mathbf{M}$ and $\mathbf{N}$ are given by

$$\mathbf{M}=\begin{bmatrix}\mathbf{Id}_3 & 0\\ 0 & 0\end{bmatrix}\quad\text{and}\quad\mathbf{N}=\begin{bmatrix}0 & \mathbf{Id}_3\\ 0 & 0\end{bmatrix}.\tag{14}$$

Eqs. (9) or (12) and (13) form an eigenvalue problem. A given (squared) frequency $\omega_\alpha^2(\mathbf{k})$ is called an eigenvalue if Eqs. (9) and (13) admit a non-zero solution. The associated non-zero solution $\phi_\alpha(x_3,\mathbf{k})$, called an eigenfunction, represents a propagating wave mode of the sandwich structure. The dynamic properties of the sandwich structure depend critically on what are the eigenvalues and the eigenfunctions, and how they depend on the in-plane wavevector $\mathbf{k}$ and structural properties $\mathbf{L}_i,\rho_i,h_i$ $(i=1,2,3)$.

We have the following result from Atkinson (1964, Theorem 9.2.1) and Zettl (2005) that asserts the existence of eigenvalues and eigenfunctions.

Theorem 1. *Consider the Hamiltonian system (9) or (12) and (13). For a given in-plane wavevector $\mathbf{k}\in\Gamma_0$, there exist infinitely many eigenvalues $\omega_\alpha^2(\mathbf{k})$ $(\alpha=0,1,2,\ldots)$ with no finite accumulation point*

$$0\leqslant\omega_0^2(\mathbf{k})\leqslant\omega_1^2(\mathbf{k})\leqslant\omega_2^2(\mathbf{k})\leqslant\cdots\nearrow+\infty\tag{15}$$

such that Eqs. (9) and (13) admit non-zero solutions, where $\omega_\alpha^2(\mathbf{k})$ $(\alpha=0,1,2,\ldots)$ are repeated according to their multiplicity. Further, each branch of the dispersion relations $\mathbf{k}\mapsto\omega_\alpha(\mathbf{k})$ is a continuous function of $\mathbf{k}\in\Gamma_0$.

To calculate the eigenvalues and eigenvectors explicitly, we note that $\mathbf{H}(\omega,\mathbf{k})$ in Eq. (10) depends on x_3, and specifically, $\mathbf{H}(\omega,\mathbf{k})$ is equal to

$$\begin{cases}\mathbf{H}_1(\omega,\mathbf{k}) & \text{if }x_3\in(0,h_1),\\ \mathbf{H}_2(\omega,\mathbf{k}) & \text{if }x_3\in(h_1,h_1+h_2),\\ \mathbf{H}_3(\omega,\mathbf{k}) & \text{if }x_3\in(h_1+h_2,h),\end{cases}\tag{16}$$

where $\mathbf{H}_i(\omega,\mathbf{k})$ $(i=1,2,3)$ are independent of x_3, see Eqs. (5) and (10). Recall that for a square matrix X,

$$\exp(X)=\sum_{n=0}^{\infty}\frac{X^n}{n!},\ \ \cos(X)=\sum_{n=0}^{\infty}\frac{(-1)^nX^{2n}}{(2n)!},\ \ \sin(X)=\sum_{n=0}^{\infty}\frac{(-1)^nX^{2n+1}}{(2n+1)!}.\tag{17}$$

For given ω and $\mathbf{k}$, let $\phi(x_3,\omega,\mathbf{k})$ be a solution of Eqs. (9) and (13) and denote by $\phi_0\in\mathbb{C}^6$ the boundary value of $\phi(x_3,\omega,\mathbf{k})$ at $x_3=0$. From the theory of first-order differential equations (Coddington and Levinson, 1955), we can express $\phi(x_3,\omega,\mathbf{k})$ as

$$\phi(x_3,\omega,\mathbf{k})=\begin{cases}\exp[x_3\mathbf{H}_1(\omega,\mathbf{k})]\phi_0 & \text{if }x_3\in[0,h_1],\\ \exp[(x_3-h_1)\mathbf{H}_2(\omega,\mathbf{k})]\exp[h_1\mathbf{H}_1(\omega,\mathbf{k})]\phi_0 & \text{if }x_3\in[h_1,h_1+h_2],\\ \exp[(x_3-h_1-h_2)\mathbf{H}_1(\omega,\mathbf{k})]\exp[h_2\mathbf{H}_2(\omega,\mathbf{k})]\exp[h_1\mathbf{H}_1(\omega,\mathbf{k})]\phi_0 & \text{if }x_3\in[h_1+h_2,h].\end{cases}\tag{18}$$

In particular, we have

$$\phi(h,\omega,\mathbf{k})=\mathbb{T}(\omega,\mathbf{k})\phi_0=\mathbb{T}(\omega,\mathbf{k})\phi(0,\omega,\mathbf{k}),\tag{19}$$

where

$$\mathbb{T}(\omega,\mathbf{k})=\exp[h_3\mathbf{H}_3(\omega,\mathbf{k})]\exp[h_2\mathbf{H}_2(\omega,\mathbf{k})]\exp[h_1\mathbf{H}_1(\omega,\mathbf{k})]\tag{20}$$

is referred to as the global *transfer matrix* and $\exp[h_i\mathbf{H}_i(\omega,\mathbf{k})]$ is referred to as the local transfer matrix associated with layer i $(i=1,2,3)$. From Eqs. (13) and (19), we see that Eqs. (9) and (13) admit a non-zero solution if, and only if

$$\operatorname{rank}(\mathbb{T}(\omega,\mathbf{k})\mathbf{M}-\mathbf{N})<6. \tag{21}$$

Direct calculations reveal that

$$\mathbb{T}(\omega,\mathbf{k})\mathbf{M}-\mathbf{N}=\begin{bmatrix}\mathbb{T}_{11} & -\mathbf{Id}_3\\ \mathbb{T}_{21} & 0\end{bmatrix},\quad \text{where}\quad \begin{bmatrix}\mathbb{T}_{11} & \mathbb{T}_{12}\\ \mathbb{T}_{21} & \mathbb{T}_{22}\end{bmatrix}=\mathbb{T}. \tag{22}$$

Thus,

$$6-\operatorname{rank}(\mathbb{T}(\omega,\mathbf{k})\mathbf{M}-\mathbf{N})=3-\operatorname{rank}(\mathbb{T}_{21}(\omega,\mathbf{k})), \tag{23}$$

and the geometric multiplicity of each eigenvalue $\omega_\alpha^2(\mathbf{k})$ is at most three.

Eq. (21) completely determines all the eigenvalues $\omega_\alpha^2(\mathbf{k})$ and their dependence on the in-plane wavevector $\mathbf{k}$ and structural properties $\mathbf{L}_i,\rho_i,h_i$ $(i=1,2,3)$. Thus, for given $\mathbf{L}_i,\rho_i,h_i$ $(i=1,2,3)$, we are able to calculate all dispersion relations $\mathbf{k}\mapsto\omega_\alpha(\mathbf{k})$ $(\alpha=0,1,\ldots)$. We do so numerically for the following example.

Example 2.1. In this example, we specify that the material of the top and bottom layers is aluminum (isotropic, Young's modulus $E_1=E_3=70$ Gpa, Poisson's ratio $\nu_1=\nu_3=0.35$, density 2700 kg/m^3), and that the material of the middle layer is a kind of foam (isotropic, Young's modulus $E_2=0.12$ Gpa, Poisson's ratio $\nu_2=0.31$, density 100 kg/m^3). The thicknesses of bottom, middle and top layer are $h_1=2.5$ mm, $h_2=50$ mm and $h_3=h_1=2.5$ mm.

Let $\mathbf{k}=k_1\mathbf{e}_1,\lambda=2\pi/k_1$ be the wavelength and $h=55$ mm be the total thickness of the sandwich structure. For an isotropic material, the Lamé constants μ_i,λ_i can be expressed as [1]

$$\mu_i=\frac{E_i}{2(1+\nu_i)},\quad \lambda_i=\frac{E_i\nu_i}{(1+\nu_i)(1-2\nu_i)},$$

and hence the matrices $\mathbf{Q}_i,\mathbf{R}_i,\mathbf{T}_i$ in Eq. (5) can be written as $(\mathbf{k}=k_1\mathbf{e}_1)$

$$\mathbf{T}_i=\begin{bmatrix}\mu_i & 0 & 0\\ 0 & \mu_i & 0\\ 0 & 0 & 2\mu_i+\lambda_i\end{bmatrix},\ \mathbf{R}_i=\begin{bmatrix}0 & 0 & \lambda_i\\ 0 & 0 & 0\\ \mu_i & 0 & 0\end{bmatrix},\ \mathbf{Q}_i=\begin{bmatrix}2\mu_i+\lambda_i & 0 & 0\\ 0 & \mu_i & 0\\ 0 & 0 & \mu_i\end{bmatrix}. \tag{24}$$

From Eqs. (10) and (16), direct calculations reveal that

$$\mathbf{H}_i(\omega,k_1\mathbf{e})=\begin{bmatrix}0 & 0 & -ik_1 & \frac{1}{\mu_i} & 0 & 0\\ 0 & 0 & 0 & 0 & \frac{1}{\mu_i} & 0\\ -ik_1\frac{\lambda_i}{2\mu_i+\lambda_i} & 0 & 0 & 0 & 0 & \frac{1}{2\mu_i+\lambda_i}\\ \frac{4\mu_i(\mu_i+\lambda_i)}{2\mu_i+\lambda_i}k_1^2-\rho_i\omega^2 & 0 & 0 & 0 & 0 & -ik_1\frac{\lambda_i}{2\mu_i+\lambda_i}\\ 0 & \mu_ik_1^2-\rho_i\omega^2 & 0 & 0 & 0 & 0\\ 0 & 0 & -\rho_i\omega^2 & -ik_1 & 0 & 0\end{bmatrix}. \tag{25}$$

Plugging Eq. (25) into Eq. (20), we calculate the transfer matrix $\mathbb{T}(\omega,\mathbf{k})$ and solve Eq. (21) for natural frequencies $\omega_\alpha(\mathbf{k})$. The results are shown in Fig. 2, where each "•" denotes a natural frequency $\omega_\alpha(k_1\mathbf{e}_1)$. Since no theoretical but numerical approximation has been introduced in the transfer matrix method, these results are referred to as the *exact* results subsequently.

The above approach of transfer matrix, though exact and theoretically complete, has a few disadvantages. First of all, numerically searching eigenvalues $\omega_\alpha^2(\mathbf{k})$ is not at all trivial since the transfer matrix $\mathbb{T}(\omega,\mathbf{k})$ is a transcendental (more specifically, trigonometric) function of ω. The reader may appreciate the difficulty from a recent review on "nineteen dubious ways to compute the exponential of a matrix" (Moler and Loan, 2003). The numerical method we have chosen to calculate the natural frequencies $\omega_\alpha(\mathbf{k})$ is by "brute force". That is, for each given $\mathbf{k}$, we divide ω-interval $[0,4\times10^5]$ s^{-1} into hundreds of small disjoint subintervals. In each of these small subintervals, we then search the value of ω such that the matrix $\mathbb{T}_{21}(\omega,\mathbf{k})$ becomes singular. Since the smallness of the subintervals is limited, from Theorem 1 we see that many eigenvalues must have been missed in Fig. 2, especially in places where various branches of $\mathbf{k}\mapsto\omega_\alpha(\mathbf{k})$ are close to each other. Further, without solving Eq. (21), one can hardly infer any qualitative information about the dispersion relations, which is however desired in practical applications. Finally, without solving Eq. (21) and evaluating the corresponding eigenfunction (18), this approach cannot provide us any physical intuition about the mode shape, strain and stress profiles.

3. Long wavelength limit

Two features of the dispersion relation shown in Fig. 2 are noteworthy in the long wavelength regime. (i) Except the lowest three branches, every branch $\omega_\alpha(k_1\mathbf{e}_1)$ starts horizontally from $k_1=0$. This is emphasized in Fig. 3 by replotting Fig. 2 for (h/λ)-interval $[0,0.1]$. This feature means the group velocities of these modes, $\partial\omega_\alpha(k_1\mathbf{e}_1)/\partial k_1$, vanish at $k_1=0$, and so high dissipation rates are expected at these frequencies $\omega_\alpha(0)$ in a practical situation. Similar tendency has been observed for an isotropic homogeneous slab (Mindlin, 1960). (ii) If we zoom in the long wavelength and low frequency regime and replot the lowest three branches of $k_1\mapsto\omega_\alpha(k_1\mathbf{e}_1)$ $(\alpha=0,1,2)$ in Fig. 4, we see that $k_1\mapsto\omega_\alpha(k_1\mathbf{e}_1)$ $(\alpha=1,2)$ are initially linear, while the lowest branch $k_1\mapsto\omega_0(k_1\mathbf{e}_1)$ is initially quadratic but tends to be linear as the wavelength decreases. In this section, we seek explanations to these two features, and in particular we give formulas to calculate the frequencies $\omega_\alpha(0)$ for $\alpha>2$ and the slopes of the (approximately) linear functions $k_1\mapsto\omega_\alpha(k_1\mathbf{e}_1)$ at $k_1=0$ for $\alpha=0,1,2$.

3.1. A formula for $\omega_\alpha(0)$

It is convenient to express the transfer matrix in a block matrix form as the Hamiltonian matrix $\mathbf{H}$ in Eq. (10). To this end, let $\Psi(x_3)=\exp(x_3\mathbf{H}_i(\omega,\mathbf{k}))$ be a 6×6 matrix solution of the ordinary differential equation:

$$\Psi'(x_3)=\mathbf{H}_i(\omega,\mathbf{k})\Psi(x_3), \tag{26}$$

where $\mathbf{H}_i(\omega,\mathbf{k})$ $(i=1,2,3)$ are given by Eq. (16). We try a 6×3 matrix solution of the following form:

$$\Phi(x_3)=\begin{bmatrix}\mathbf{Id}_3\\ (\mathbf{T}_i+i|\mathbf{k}|\mathbf{R}_i^T)\end{bmatrix}\exp(\mathbf{K}x_3), \tag{27}$$

where $\mathbf{K}\in\mathbb{C}^{3\times3}$ is to be determined. Inserting Eq. (27) into Eq. (26) we obtain

$$\mathbf{H}_i(\omega,\mathbf{k})\begin{bmatrix}\mathbf{Id}_3\\ (\mathbf{T}_i\mathbf{K}+i|\mathbf{k}|\mathbf{R}_i^T)\end{bmatrix}=\begin{bmatrix}\mathbf{Id}_3\\ (\mathbf{T}_i\mathbf{K}+i|\mathbf{k}|\mathbf{R}_i^T)\end{bmatrix}\mathbf{K}, \tag{28}$$

which is equivalent to the following *algebraic Riccati equation* for $\mathbf{K}$ (see Lancaster and Rodman, 1995):

$$\mathbf{T}_i\mathbf{K}^2-i|\mathbf{k}|(\mathbf{R}_i+\mathbf{R}_i^T)\mathbf{K}+(|\mathbf{k}|^2\mathbf{Q}_i-\rho\omega^2\mathbf{Id}_3)=0. \tag{29}$$

If Eq. (29) admits two solutions $\mathbf{K}_1$ and $\mathbf{K}_2$ with $\det(\mathbf{K}_1-\mathbf{K}_2)\neq0$, one can verify that

$$[\,\Phi_1(x_3)\quad\Phi_2(x_3)\,][\,\Phi_1(0)\quad\Phi_2(0)\,]^{-1} \tag{30}$$

satisfy Eq. (26) and is equal to $\mathbf{Id}_6$ at $x_3=0$, where

$$[\,\Phi_1(x_3)\ \ \Phi_2(x_3)\,]=\begin{bmatrix}\exp(x_3\mathbf{K}_1) & \exp(x_3\mathbf{K}_2)\\ (\mathbf{T}_i\mathbf{K}_1+i|\mathbf{k}|\mathbf{R}_i^T)\exp(x_3\mathbf{K}_1) & (\mathbf{T}_i\mathbf{K}_2+i|\mathbf{k}|\mathbf{R}_i^T)\exp(x_3\mathbf{K}_2)\end{bmatrix}. \tag{31}$$

[1] The Lamé constants λ_i, always with a subscript in this paper, should not be confused with the wavelength λ.

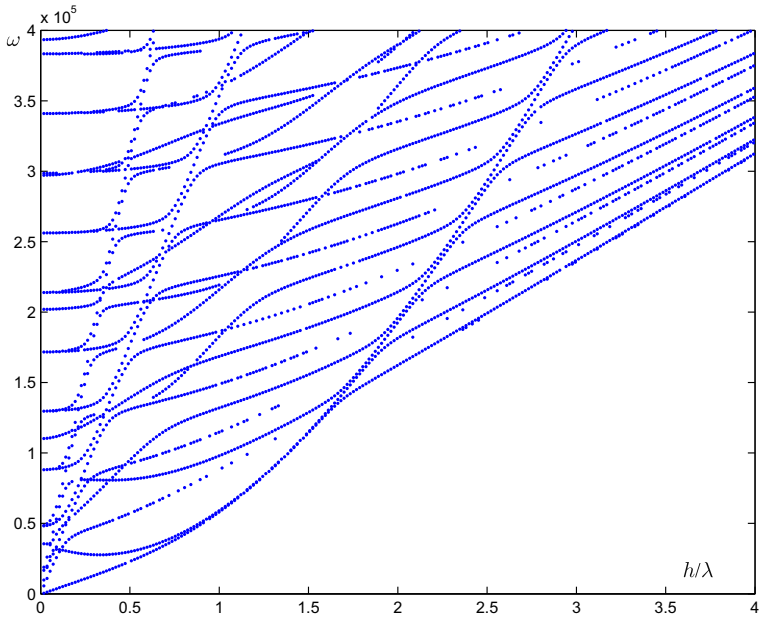

Fig. 2. The spectrum of the sandwich structure specified in Example 2.1. Each "•" denotes a natural frequency $\omega_\alpha(\mathbf{k})$ determined by Eq. (21). The figure for (h/λ)-interval [0,0.1] is replotted in Fig. 3.

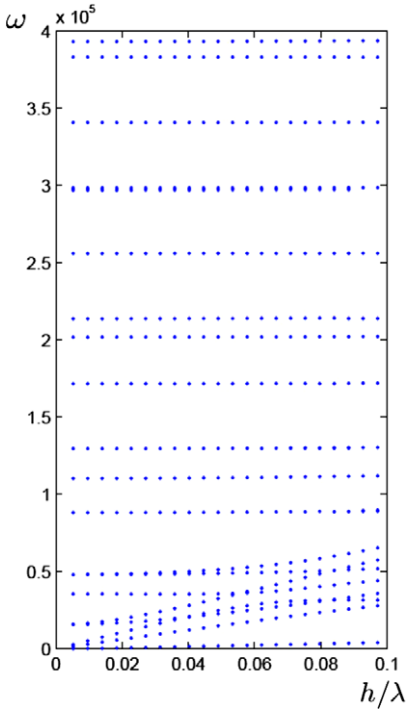

Fig. 3. The spectrum of the sandwich structure in the long wavelength regime. Each "•" denotes a natural frequency determined by Eq. (21).

Therefore, the expression in Eq. (30) must be equal to $\Psi(x_3) = \exp(x_3\mathbf{H}_i(\omega,\mathbf{k}))$.

We remark that an explicit block form of the transfer matrix as in Eq. (30) is useful in calculating the eigenvalues and eigenfunctions, including the cases for which the boundary conditions are different from present ones. In the case of $\mathbf{k}=0$, clearly $\pm\mathbf{K} = \pm\sqrt{\rho_i\omega^2}\mathbf{T}_i^{-1/2}$ satisfy Eq. (29). By Eqs. (30) and (31), straightforward calculations reveal that (cf., Eq. (17))

$$\exp[h_i\mathbf{H}_i(\omega,0)] = \begin{bmatrix} \cos(\widetilde{\mathbf{T}}_i) & \frac{\mathbf{T}_i^{-1/2}}{\sqrt{\rho_i\omega^2}}\sin(\widetilde{\mathbf{T}}_i) \\ -\sqrt{\rho_i\omega^2}\mathbf{T}_i^{1/2}\sin(\widetilde{\mathbf{T}}_i) & \cos(\widetilde{\mathbf{T}}_i) \end{bmatrix}, \tag{32}$$

where $\widetilde{\mathbf{T}}_i = [\rho_i(h_i\omega)^2]^{-1}\mathbf{T}_i$. To find ω that satisfies Eq. (21), by Eqs. (22) and (23), we see that only $\mathbb{T}_{21}$ is relevant. From Eqs. (32) and (20), we have

$$\begin{aligned}\mathbb{T}_{21}(\omega,0) = &-\sqrt{\rho_3\omega^2}\mathbf{T}_3^{1/2}\sin(\widetilde{\mathbf{T}}_3^{-1/2})\Big[\cos(\widetilde{\mathbf{T}}_2^{-1/2})\cos(\widetilde{\mathbf{T}}_1^{-1/2}) \\ &-\mathbf{T}_2^{-1/2}\sqrt{\frac{\rho_1}{\rho_2}}\sin(\widetilde{\mathbf{T}}_2^{-1/2})(\mathbf{T}_1^{1/2})\sin(\widetilde{\mathbf{T}}_1^{-1/2})\Big] \\ &+\cos(\widetilde{\mathbf{T}}_3^{-1/2})\Big[-\sqrt{\rho_2\omega^2}\mathbf{T}_2^{1/2}\sin(\widetilde{\mathbf{T}}_2^{-1/2})\cos(\widetilde{\mathbf{T}}_1^{-1/2}) \\ &-\sqrt{\rho_1\omega^2}\cos(\widetilde{\mathbf{T}}_2^{-1/2})\mathbf{T}_1^{1/2}\sin(\widetilde{\mathbf{T}}_1^{-1/2})\Big].\end{aligned} \tag{33}$$

We remark that explicit expression for $\mathbb{T}_{21}$ as in Eq. (33) is possible for non-zero wavevectors, upon which we do not elaborate here.

For an isotropic material with Lamé constants μ_i, λ_i, we have $\mathbf{T}_i$ given by Eq. (24) and

$$\widetilde{\mathbf{T}}_i^{-1/2} = \mathrm{diag}\left[h_i\omega\sqrt{\frac{\rho_i}{\gamma_{i1}}}, h_i\omega\sqrt{\frac{\rho_i}{\gamma_{i2}}}, h_i\omega\sqrt{\frac{\rho_i}{\gamma_{i3}}}\right],$$

where $\gamma_{i1} = \gamma_{i2} = \mu_i$ and $\gamma_{i3} = 2\mu_i + \lambda_i$ for $i = 1,2,3$. Thus, $\mathbb{T}_{12}(\omega,0)/\omega$ in Eq. (33) is a 3×3 diagonal matrix with diagonal elements given by ($j = 1,2,3$)

$$\begin{aligned}\Lambda_j(\omega) = &\sin\left(h_3\omega\sqrt{\frac{\rho_3}{\gamma_{3j}}}\right)\left[-\sqrt{\rho_3\gamma_{3j}}\cos\left(h_2\omega\sqrt{\frac{\rho_2}{\gamma_{2j}}}\right)\cos\left(h_1\omega\sqrt{\frac{\rho_1}{\gamma_{1j}}}\right)\right. \\ &\left.+\sqrt{\frac{\rho_3\rho_1\gamma_{3j}\gamma_{1j}}{\rho_2\gamma_{2j}}}\sin\left(h_2\omega\sqrt{\frac{\rho_2}{\gamma_{2j}}}\right)\sin\left(h_1\omega\sqrt{\frac{\rho_1}{\gamma_{1j}}}\right)\right] \\ &+\cos\left(h_3\omega\sqrt{\frac{\rho_3}{\gamma_{3j}}}\right)\left[-\sqrt{\rho_2\gamma_{2j}}\sin\left(h_2\omega\sqrt{\frac{\rho_2}{\gamma_{2j}}}\right)\cos\left(h_1\omega\sqrt{\frac{\rho_1}{\gamma_{1j}}}\right)\right. \\ &\left.-\sqrt{\rho_1\gamma_{1j}}\cos\left(h_2\omega\sqrt{\frac{\rho_2}{\gamma_{2j}}}\right)\sin\left(h_1\omega\sqrt{\frac{\rho_1}{\gamma_{1j}}}\right)\right].\end{aligned} \tag{34}$$

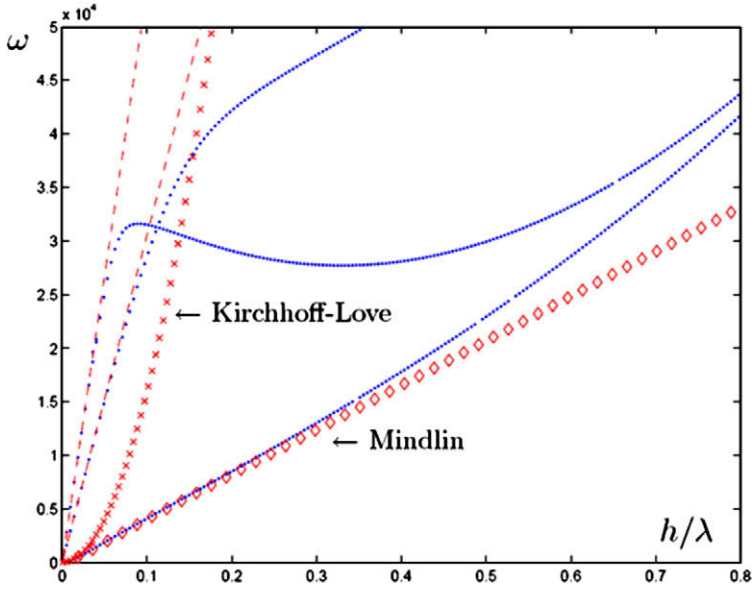

Fig. 4. The lowest three branches of the dispersion relations in the long wavelength and low frequency regime. (•) The transfer matrix method; (– –) perturbation method described in Section 3.2, see Eq. (36); (×) the Kirchhoff–Love plate theory, see Eq. (45); (◇) the Mindlin plate theory, see Eq. (52).

Thus, a non-zero ω such that Eq. (21) holds if and only if $\Lambda_j(\omega)$ in Eq. (34) vanishes for some $j \in \{1,2,3\}$. For the sandwich structure specified in Example 2.1, the graphs of Λ_j $(j=1,2,3)$ are shown in Fig. 5 for ω-interval $[0, 4\times 10^5]$ s^{-1}. The inset in Fig. 5 is a zoom-in of the graphs for ω-interval $[0, 0.5\times 10^5]$ s^{-1}. The intersections of these curves with the horizontal axis are the natural frequencies $\omega_\alpha(0)(\alpha = 0,1,\ldots)$ of the sandwich structure for $\mathbf{k}=0$. Compared with Fig. 3, we see that these natural frequencies agree well with the numerical results of the transfer matrix method.

In particular, if the sandwich structure is homogeneous, i.e., $\mu_i, \lambda_i, \rho_i = \mu_0, \lambda_0, \rho_0$ for all $i=1,2,3$, Eq. (34) vanishing for some $j \in \{1,2,3\}$ is equivalent to

$$\sin\left(h\omega\sqrt{\frac{\rho_0}{\mu_0}}\right)=0 \quad \text{or} \quad \sin\left(h\omega\sqrt{\frac{\rho_0}{2\mu_0+\lambda_0}}\right)=0.$$

We have thus recovered the well-known results for the Rayleigh–Lamb waves with zero in-plane wavevector (Lamb, 1917).

It is further worthwhile noticing a scaling relation between $\omega_\alpha(0)$ and h_1, h_2, h_3. From Eq. (33), we see that $\mathbb{T}_{12}(\omega,0)/\omega$ is invariant under the following transformation

$$h_1 \to a h_1, \quad h_2 \to a h_2, \quad h_3 \to a h_3, \quad \omega \to \frac{\omega}{a} \qquad \forall a > 0.$$

Therefore, if the sandwich structure is uniformly expanded a times, the limit points $\omega_\alpha(0)$ of dispersion relations on ω-axis shrink uniformly $1/a$ times. This fact is self-evident for isotropic materials, see

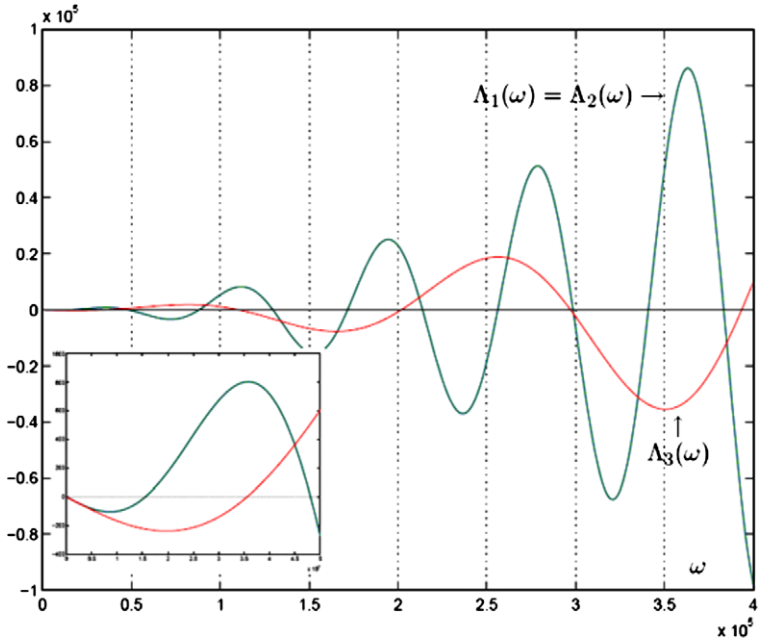

Fig. 5. Graphs of $\Lambda_j(\Omega)$ in Eq. (34) for the sandwich structure in Example 2.1. The inset is a zoom-in for ω-interval $[0, 0.5\times 10^5]$ s^{-1}.

Eq. (34). We point out that it also holds for general anisotropic materials, see Eqs. (32) and (20).

3.2. Dispersion relations of the lowest three branches

We now discuss the lowest three branches around $\mathbf{k}=0$, see Fig. 4. It is not surprising that from the bottom to top, they correspond to the out-of-plane flexural modes, the in-plane transverse (shear) modes, and the in-plane longitudinal modes. Since the wavelength of these modes are much larger than the thickness of the sandwich structure, the sandwich structure behave almost like a "uniform" slab, i.e., the corresponding eigenfunction $\phi_\alpha(x_3,\omega,\mathbf{k})$ $(\alpha=0,1,2)$ of Eqs. (9) and (13) are independent of x_3 to the zeroth-order approximations.

From the viewpoint of perturbation theory (Kato, 1966), we may expand the dispersion relations $\omega_\alpha(\mathbf{k})$ in power series in $\mathbf{k}$. To find the coefficients in these expansions, we first expand the matrix $\mathbb{T}_{21}(\omega,\mathbf{k})$ as

$$\frac{1}{h|\mathbf{k}|^2}\mathbb{T}_{21}(\omega,\mathbf{k})=\sum_{i=1}^{3}[\theta_i(\mathbf{Q}_i-\mathbf{R}_i\mathbf{T}_i^{-1}\mathbf{R}_i^T)-\rho_i\theta_i v^2\mathbf{Id}_3]+\frac{1}{2}|\mathbf{k}|h\mathbf{C}(v)+\frac{1}{6}|\mathbf{k}|^2h^2\mathbf{D}(v)+\cdots, \tag{35}$$

where $\theta_i=h_i/h$ $(i=1,2,3)$ are the volume fractions of layer-i, $v=\omega/|\mathbf{k}|$ is the phase speed, and $\mathbf{C}(v),\mathbf{D}(v)$ are the higher order coefficient matrices. If higher order terms of $\mathbb{T}_{12}/h|\mathbf{k}|^2$ are neglected and the sandwich structure in Example 2.1 is considered, the values of v or ω such that $\mathbb{T}_{12}$ becomes singular can be immediately read off from Eqs. (25) and (35). That is $(\mathbf{k}=k_1\mathbf{e}_1)$,

$$\begin{cases}\frac{\omega_0(k_1\mathbf{e}_1)}{k_1}=v_0(k_1\mathbf{e}_1)=0,\\ \frac{\omega_1(k_1\mathbf{e}_1)}{k_1}=v_1(k_1\mathbf{e}_1)=\sqrt{\frac{\mu_e}{\rho_e}},\\ \frac{\omega_2(k_1\mathbf{e}_1)}{k_1}=v_2(k_1\mathbf{e}_1)=\sqrt{\frac{\widetilde{E}_e}{\rho_e}},\end{cases} \tag{36}$$

where the effective density $\rho_e=\sum_{i=1}^3\theta_i\rho_i$, the effective shear modulus $\mu_e=\sum_{i=1}^3\theta_i\mu_i$, the effective modified Young's modulus $\widetilde{E}_e=\sum_{i=1}^3\theta_i\widetilde{E}_i$, and the modified Young's modulus $\widetilde{E}_i$ is given by

$$\widetilde{E}_i=\frac{E_i}{1-\nu_i^2}=\frac{4\mu_i(\mu_i+\lambda_i)}{2\mu_i+\lambda_i}.$$

The straight lines of $\omega_1(k_1\mathbf{e})=k_1\sqrt{\mu_e/\rho_e}$ and $\omega_2(k_1\mathbf{e})=k_1\sqrt{\widetilde{E}_e/\rho_e}$ are plotted in Fig. 4 in dashed lines "– –", whereas the exact results of the transfer matrix method are plotted in "•" markers. One can see that Eq. (36) agrees well with the exact results when $h/\lambda\lesssim 0.1$.

A remark is in order here regarding N-layers of anisotropic materials. In these situations, Eq. (35) remains valid for calculating the slopes of the lowest three branches of the dispersion relations $\mathbf{k}\mapsto\omega_\alpha(\mathbf{k})$ to the first order of $|\mathbf{k}|$. Further, by direct calculations it has been shown that (Ting, 1996, Chapter 6) for general anisotropic materials, the matrices $\mathbf{Q}_i-\mathbf{R}_i\mathbf{T}_i^{-1}\mathbf{R}_i^T$ can all be written as $(i=1,\ldots,N)$

$$\mathbf{Q}_i-\mathbf{R}_i\mathbf{T}_i^{-1}\mathbf{R}_i^T=\begin{bmatrix}*&*&0\\*&*&0\\0&0&0\end{bmatrix},$$

where $*$ denotes potential non-zero entries and the upper 2×2 diagonal block is positive definite. Thus, the lowest three branches of the dispersion relations, even in these general situations, consist of one out-of-plane flexural modes and two in-plane modes. The slopes of these dispersion relations can be conveniently calculated by solving the secular equation

$$\det\left[\sum_{i=1}^{N}\theta_i(\mathbf{Q}_i-\mathbf{R}_i\mathbf{T}_i^{-1}\mathbf{R}_i^T)-\rho_e v^2\mathbf{Id}_3\right]=0. \tag{37}$$

We can consider higher order terms in Eq. (35) to find higher order correction on the dispersion relation $k_1\mapsto\omega_0(k_1\mathbf{e}_1)$ in the long wavelength regime. To demonstrate the idea, let us consider a homogeneous layer of thickness h, elasticity tensor $\mathbf{L}_0$, density ρ_0, and so the corresponding matrices $\mathbf{T}_0,\mathbf{R}_0,\mathbf{Q}_0$ are well defined as by Eq. (5) for $\mathbf{L}=\mathbf{L}_0$. Let

$$\widetilde{\mathbf{Q}}(v)=(\mathbf{Q}_0-\mathbf{R}_0\mathbf{T}_0^{-1}\mathbf{R}_0^T)-\rho_0 v^2\mathbf{Id}_3\quad\text{and}\quad\widetilde{\mathbf{A}}=-i\mathbf{T}_0^{-1}\mathbf{R}_0^T. \tag{38}$$

Then tedious but straightforward algebraic calculations reveal that the matrices $\mathbf{C}(v),\mathbf{D}(v)$ in the expansion (35) can be written as (Mathematica will help)

$$\mathbf{C}(v)=\widetilde{\mathbf{Q}}(v)\widetilde{\mathbf{A}}+\widetilde{\mathbf{A}}^T\widetilde{\mathbf{Q}}(v) \tag{39}$$

and

$$\mathbf{D}(v)=\widetilde{\mathbf{Q}}(v)\mathbf{A}_0^2+\widetilde{\mathbf{A}}^T\widetilde{\mathbf{Q}}\widetilde{\mathbf{A}}+\widetilde{\mathbf{Q}}(v)\mathbf{T}_0^{-1}\widetilde{\mathbf{Q}}(v)+(\widetilde{\mathbf{A}}^T)^2\widetilde{\mathbf{Q}}(v). \tag{40}$$

As is well known, the phase speed v of the flexural modes is proportional to $|\mathbf{k}|$ for a homogeneous layer, see e.g. Landau and Lifshitz (1986). So, if we keep terms up to $|\mathbf{k}|^2$ in the expansion (35), we have

$$\frac{1}{h|\mathbf{k}|^2}\mathbb{T}_{21}(\omega,\mathbf{k})\approx\widetilde{\mathbf{Q}}(v)+\frac{h|\mathbf{k}|}{2}\mathbf{C}(0)+\frac{h^2|\mathbf{k}|^2}{6}\mathbf{D}(0). \tag{41}$$

If in particular $\mathbf{L}_0$ is an isotropic elasticity tensor with Lamé constants μ_0,λ_0 or Young's modulus E_0 and Poisson's ratio ν_0, by Eqs. (25) and (41) can be written as $(\mathbf{k}=k_1\mathbf{e}_1$ and $\widetilde{E}_0=E_0/(1-\nu_0^2))$

$$\frac{1}{hk_1^2}\mathbb{T}_{21}(\omega,k_1\mathbf{e}_1)\approx\begin{bmatrix}\widetilde{E}_0\left(1+\frac{h^2k_1^2}{3}\right)-\rho_0v^2&0&-i\frac{hk_1}{2}\widetilde{E}_0\\0&\mu_0-\rho_0v^2&0\\-i\frac{hk_1}{2}\widetilde{E}_0&0&-\frac{h^2k_1^2}{6}\widetilde{E}_0-\rho_0v^2\end{bmatrix}.$$

Therefore, $\frac{1}{hk_1^2}\mathbb{T}_{21}(\omega,k_1\mathbf{e}_1)$ is singular if

$$\mu_0-\rho_0v^2=0\quad\text{or}\quad-\left(\widetilde{E}_0\left(1+\frac{h^2k_1^2}{3}\right)-\rho_0v^2\right)\left(\frac{h^2k_1^2}{6}\widetilde{E}_0+\rho_0v^2\right)+\frac{\widetilde{E}_0^2h^2k_1^2}{4}=0. \tag{42}$$

Neglecting higher-order terms in the latter of Eq. (42), we have

$$v\approx hk_1\sqrt{\frac{\widetilde{E}_0}{12\rho_0}}=k_1\sqrt{\frac{D_0}{\rho_0h}}, \tag{43}$$

where $D_0=h^3\widetilde{E}_0/12$ is the flexural rigidity of this homogeneous slab. Eq. (43) confirms the prediction of the Kirchhoff–Love plate theory. In this regard, the predictions of higher order plate theories (see e.g. Lo et al., 1977a,b) can also be achieved by including higher order terms in the expansion (35).

Unfortunately, for a heterogeneous laminated structure, say, the sandwich structure in Example 2.1, the pertinent algebra gets untractable if one attempts to calculate the higher order terms (i.e., $\mathbf{C}(v)$ and $\mathbf{D}(v)$) in Eq. (35). Nevertheless, we argue that this method in principle works for a heterogeneous laminated structure as well as for a homogeneous slab. In fact, from the perturbation theory (Kato, 1966), this method has no limit in finding all coefficients in the power series expansion of $\omega_\alpha(\mathbf{k})$. From this viewpoint, by fitting the dispersion equation of the Mindlin plate theory (cf., Eq. (61)) with the higher order coefficients of the expansion $\omega_0(\mathbf{k})$, we can determine the "best" Mindlin shear correction factor for a heterogeneous laminated structure, see Timoshenko (1922) and Stephen (1997). Again, for the complicated algebra, an explicit example is not attempted here.

4. The lowest branch of the dispersion relations

In reality, the dynamic behavior of the sandwich structure is dictated to a large extend by the lowest branch of the dispersion relations $\mathbf{k}\mapsto\omega_0(\mathbf{k})$ (and the nearby branches if the gaps between them are small). We restrict ourselves to the sandwich structure specified in Example 2.1 in this section. By the transfer matrix method in Section 2, we numerically calculate the lowest branch of the dispersion relation which is shown in the top figure of Fig. 6, see also Fig. 2. Typical mode shapes corresponding to the lowest branch, also calculated by the transfer matrix method, are shown in the bottom of Fig. 6. The numbers along with the mode shapes are the values of h/λ. According to the mode shapes, the (h/λ)-interval $[0,4]$ can be roughly divided into four regimes labeled by "flexural", "flexural-dilatational", "vertical shear" and "horizontal shear" on the top of Fig. 6. Below we present some simple physical models capable of predicting the lowest dispersion relation in various regimes.

4.1. Flexural modes

As suggested by the first mode shape in Fig. 6, the sandwich structure flexes as a uniform plate when the wavelength is large compared with the thickness of the plate. We therefore model the sandwich structure by a homogeneous "equivalent" plate with an effective flexural rigidity (Christensen, 1979)

$$D_e=\int_0^h\left(x_3-\frac{h}{2}\right)^2\widetilde{E}(x_3)dx_3, \tag{44}$$

where $\widetilde{E}(x_3)$ is the modified Young modulus, taking values of $\widetilde{E}_i=E_i/(1-\nu_i^2)$ if x_3 is in the ith layer of the sandwich structure. If the Kirchhoff–Love (thin) plate theory is used, the dispersion relation is given by (cf., Eq. (43))

$$D_e|\mathbf{k}|^4=\rho_e h\omega_0^2(\mathbf{k})\ \Rightarrow\ \omega_0(|\mathbf{k}|)=|\mathbf{k}|^2\sqrt{\frac{D_e}{\rho_e h}}, \tag{45}$$

see e.g. Landau and Lifshitz (1986) and Timoshenko and Woinowsky-Krieger (1959). The graph of Eq. (45) is shown by "×" signs in Fig. 4. One can see that it agrees well with the exact results when the wavelength is very large but deviates from the exact results considerably when the h/λ is larger than 0.02. Compared with a homogeneous plate, the valid regime of the Kirchhoff–Love plate theory is narrow, because the shear modulus of the top/bottom layers is hundreds of times larger than the middle core.

To improve the result, instead of various higher order plate theories (Lo et al., 1977a,b; Frostig and Baruch, 1994; Backström and Nilsson, 2006), we favor the engineering theory of Mindlin (1951) for its remarkable accuracy and simplicity. The Mindlin plate theory begins with the kinematic hypothesis that the in-plane displacements depend linearly on x_3, whereas the out-of-plane displacement is independent of x_3:

$$u_1=\left(x_3-\frac{h}{2}\right)\beta_1(x_1,x_2,t),\ \ u_2=\left(x_3-\frac{h}{2}\right)\beta_2(x_1,x_2,t),\ \ u_3=u_3(x_1,x_2,t). \tag{46}$$

We remark that this kinematic hypothesis is the same as that of the Kirchhoff–Love plate theory, and from the viewpoint of the perturbation theory, the resulting theory should not yield better result than that of the Kirchhoff-Love plate theory. Let $\epsilon_{ij}(\sigma_{ij})$ be the strain (stress) field, and $(\alpha=1,2)$

$$\Pi_\alpha(x_1,x_2)=h^{-1}\int_0^h\epsilon_{\alpha3}(\mathbf{x},t)dx_3\quad\left(Q_\alpha(x_1,x_2)=h^{-1}\int_0^h\sigma_{\alpha3}(\mathbf{x},t)dx_3\right) \tag{47}$$

be the transverse shear strain (shear stress) averaged over the thickness direction. A second hypothesis of the Mindlin plate theory is that $\sigma_{33}=0$ everywhere, which implies the in-plane strain–stress relations

$$\sigma_{11}=\widetilde{E}(\epsilon_{11}+\nu\epsilon_{22}),\quad \sigma_{22}=\widetilde{E}(\nu\epsilon_{11}+\epsilon_{22}),\quad \sigma_{12}=2\widetilde{E}(1-\nu)\epsilon_{12}. \tag{48}$$

Following the same procedure of Mindlin (1951), we manipulate the equations of the balance of linear momentum and obtain

$$\begin{cases} D_e\nabla^2\Phi-h\left(\frac{\partial Q_1}{\partial x_1}+\frac{\partial Q_2}{\partial x_2}\right)=I\frac{\partial^2\Phi}{\partial t^2},\\ \frac{\partial Q_1}{\partial x_1}+\frac{\partial Q_2}{\partial x_2}=\rho_e\frac{\partial^2 u_3}{\partial t^2}, \end{cases} \tag{49}$$

where $\Phi=(\partial\beta_1/\partial x_1)+(\partial\beta_2/\partial x_2)$ and $I=\int_0^h(x_3-\frac{h}{2})^2\rho(x_3)dx_3$ is the moment of inertia per unit area. In the Kirchhoff–Love plate theory, it is assumed that the rotatory inertial (i.e., the right-hand side of the first in Eq. (49)) is negligible and that the transverse shear strains $\epsilon_{\alpha3}$ $(\alpha=1,2)$ vanishes everywhere (which implies $\Phi=-\nabla^2u_3$). In the Mindlin plate theory, however, in account of the transverse shear, a third hypothesis is enforced, i.e., the average transverse shear strain and shear stress are related by

$$Q_\alpha=\mu_e'\Pi_\alpha\quad(\alpha=1,2), \tag{50}$$

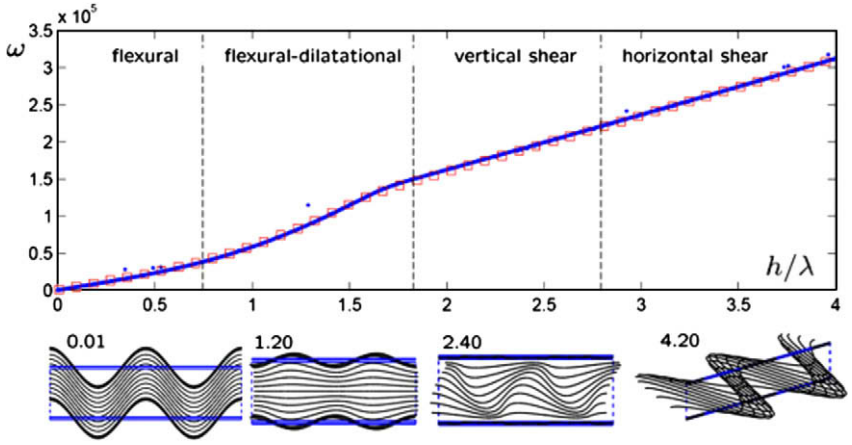

Fig. 6. The top figure shows the lowest branch of the dispersion relation of the sandwich structure in Example 2.1. The horizontal axis is roughly divided into four regimes labeled by "flexural", "flexural-dilatational", "vertical shear" and "horizontal shear". The corresponding typical mode shapes are shown in the bottom. The numbers above the mode shapes are their values of h/λ. The "□" markers show the lowest dispersion relation determined by Eq. (61).

where $\mu_e' = \eta\tilde{\mu}_e$, $\tilde{\mu}_e = (\sum_{i=1}^{3}\mu_i^{-1})^{-1}$ is the effective transverse shear modulus of the sandwich structure, and η is referred to as the correction factor, see remarks below. From Eqs. (50), (46) and (47), we have

$$\frac{\partial Q_1}{\partial x_1}+\frac{\partial Q_2}{\partial x_2}=\mu_e'(\nabla^2 u_3+\Phi).$$

Substituting it into Eq. (49), we obtain

$$\begin{cases}(D_e\nabla^2 - I\frac{\partial^2}{\partial t^2})\Phi=\rho_e h\frac{\partial^2 u_3}{\partial t^2},\\ \Phi=(\frac{\rho_e}{\mu_e'}\frac{\partial^2}{\partial t^2}-\nabla^2)u_3,\end{cases}$$

and hence

$$\left(D_e\nabla^2 - I\frac{\partial^2}{\partial t^2}\right)\left(\frac{\rho_e}{\mu_e'}\frac{\partial^2}{\partial t^2}-\nabla^2\right)u_3=\rho_e h\frac{\partial^2 u_3}{\partial t^2}. \tag{51}$$

Plugging $u_3(\mathbf{x},t)=u_3^0\exp(i(\mathbf{k}\cdot\mathbf{x}+\omega t))$ into Eq. (51) yields

$$(-D_e|\mathbf{k}|^2+I\omega^2)\left(-\frac{\rho_e}{\mu_e'}\omega^2+|\mathbf{k}|^2\right)=-\rho_e h\omega^2. \tag{52}$$

In the above derivation, the correction factor η associated with the averaged transverse shear strain and shear stress seems unnecessary, while it is generally agreed in computational mechanics circles that a factor, depending on the Poisson's ratio ν, between 0.7 and 1 would give "best" result. We are not aware of a systematic way of determining the value of η from three-dimensional elasticity even for a homogeneous plate. Our explanation for the necessity of such a correction factor is the following. From the viewpoint of the perturbation theory, the kinematic hypothesis (46) prescribes that the resulting theory is a second-order one regarding the prediction of the dispersion relation $\omega_0(\mathbf{k})$, whereas the Mindlin plate theory could be right up to the fourth-order – if this factor η were chosen correctly. Therefore, we shall regard the Mindlin plate theory as an empirical model rather than a rigorously justifiable theory such as the Kirchhoff-Love plate theory.

For an isotropic homogeneous plate of Poisson's ration ν_0, the most convincing way of determining the factor η, in the authors' opinion, is by fitting the dispersion relation determined by Eq. (52) and that of the flexural modes of the Rayleigh–Lamb waves in the long wavelength limit, see Stephen (1997), who found $\eta = 5/(6-\nu_0)$. As is well known in bending theory, the transverse shear strain and stress are approximately quadratic on a cross-section, attain their maximums at the middle plane and vanish on the upper and lower free surfaces (Timoshenko, 1940, p. 112). We therefore choose the Mindlin correction factor $\eta = 5/(6-\nu_2)\approx 0.88$ for our calculations.

With the relevant parameters chosen as above, the dispersion relation determined Eq. (52) for our sandwich structure in Example 2.1 is shown in Fig. 4 in " ◊" markers. One can see that the difference between the Mindlin plate theory and the exact result is small up to $h/\lambda\approx 0.8$. But when the wavelength is further decreased, the coupled modes of the flexural top/bottom layer and the dilatational middle core (see the second mode shape in Fig. 6) take over, for which a *plate* theory is clearly not a good model.

4.2. Coupled flexure-dilatation modes

When $h/\lambda \gtrsim 0.8$, the second mode shape in Fig. 6 suggests that these modes arise from the coupling of the flexural motions of the top/bottom layers and the dilatational motions of the middle layer. Notice that in this regime the wavelength is still large compared with the thickness of the top/bottom layer. Therefore, we use the Kirchhoff–Love plate theory for the top and bottom layers but three-dimensional elasticity for the middle layer.

Following above lines, we denote by q_1 and q_2 the normal component of the traction on the interface Γ_{h_1} and $\Gamma_{h_1+h_2}$, see Fig. 1. From the Kirchhoff–Love plate theory, for the bottom and top layers we have

$$\begin{cases}-D_1\nabla^2\nabla^2 u_3(x_1,x_2,h_1,t)+q_1(x_1,x_2,t)=\rho_1 h_1\frac{\partial^2 u_3(x_1,x_2,h_1,t)}{\partial t^2},\\ -D_3\nabla^2\nabla^2 u_3(x_1,x_2,h_2+h_1,t)-q_2(x_1,x_2,t)=\rho_1 h_1\frac{\partial^2 u_3(x_1,x_2,h_1+h_2,t)}{\partial t^2},\end{cases} \tag{53}$$

where $D_1=D_3=E_1h_1^3/12(1-\nu_1^2)$ are the flexural rigidity of the bottom/top layer.For the middle layer, by three-dimensional elasticity we have (Landau and Lifshitz, 1986)

$$\mu_2\nabla^2\mathbf{u}(\mathbf{x},t)+(\mu_2+\lambda_2)\nabla(\nabla\cdot\mathbf{u}(\mathbf{x},t))=\rho_2\frac{\partial^2\mathbf{u}(\mathbf{x},t)}{\partial t^2}\quad \forall x_3\in(h_1,h_1+h_2). \tag{54}$$

On the boundaries of the middle layer Γ_{h_1} and $\Gamma_{h_1+h_2}$, we have

$$\begin{cases}q_1(x_1,x_2,t)=(2\mu_2+\lambda_2)u_{3,3}(x_1,x_2,h_1,t)+\lambda_2[u_{1,1}(x_1,x_2,h_1,t)\\ \qquad +u_{2,2}(x_1,x_2,h_1,t)],\\ q_2(x_1,x_2,t)=(2\mu_2+\lambda_2)u_{3,3}(x_1,x_2,h_1+h_2,t)+\lambda_2[u_{1,1}(x_1,x_2,h_1\\ \qquad +h_2,t)+u_{2,2}(x_1,x_2,h_1+h_2,t)].\end{cases} \tag{55}$$

Plugging

$$u_p(\mathbf{x},t)=\hat{u}_p(x_3)\exp(ik_1x_1)\exp(i\omega t)\quad (p=1,3)\ \text{ and }\ u_2(\mathbf{x},t)=0 \tag{56}$$

into Eqs. (53)–(55) and eliminating q_1, q_2, we obtain

$$\begin{cases}(2\mu_2+\lambda_2)k_1^2\hat{u}_1(x_3)-ik_1(\lambda_2+\mu_2)\hat{u}_3'(x_3)-\mu_2\hat{u}_1''(x_3)=\rho_2\omega^2\hat{u}_1(x_3),\\ \mu_2k_1^2\hat{u}_3(x_3)-ik_1(\lambda_2+\mu_2)\hat{u}_1'(x_3)-(2\mu_2+\lambda_2)\hat{u}_3''(x_3)=\rho_2\omega^2\hat{u}_3(x_3),\\ ik_1\lambda_2\hat{u}_1(h_1)+(2\mu_2+\lambda_2)\hat{u}_3'(h_1)-D_1k_1^4\hat{u}_3(h_1)+\rho_1h_1\omega^2\hat{u}_3(h_1)=0,\\ -ik_1\lambda_2\hat{u}_1(h_1+h_2)-(2\mu_2+\lambda_2)\hat{u}_3'(h_1+h_2)-D_1k_1^4\hat{u}_3(h_1+h_2)\\ \qquad +\rho_1h_1\omega^2\hat{u}_3(h_1+h_2)=0.\end{cases} \tag{57}$$

We ignore the effects of the transfer shear on the in-plane motion of the middle layer. More specifically, setting $u_1''(x_3)=0$ for all $x_3\in[h_1,h_1+h_2]$ and by the first equation in Eq. (57) we have

$$\hat{u}_1(x_3)=\frac{ik_1(\lambda_2+\mu_2)}{(2\mu_2+\lambda_2)k_1^2-\rho_2\omega^2}\hat{u}_3'(x_3). \tag{58}$$

Eliminating $\hat{u}_1$ in the last three equations in Eq. (57), we arrive at

$$\begin{cases}\hat{u}_3''(x_3)=\beta_1^2\hat{u}_3(x_3),\\ \hat{u}_3'(h_1)-\beta_2\hat{u}_3(h_1)=0,\\ \hat{u}_3'(h_1+h_2)+\beta_2\hat{u}_3(h_1+h_2)=0,\end{cases} \tag{59}$$

where

$$\beta_1^2=\frac{(\mu_2k_1^2-\rho_2\omega^2)[(2\mu_2+\lambda_2)k_1^2-\rho_2\omega^2]}{(3\mu_2^2+2\mu_2\lambda_2)k_1^2-(2\mu_2+\lambda_2)\rho_2\omega^2}\quad\text{and}\quad\beta_2=\frac{[(2\mu_2+\lambda_2)k_1^2-\rho_2\omega^2](D_1k_1^4-\rho_1h_1\omega^2)}{(4\mu_2^2+3\mu_2\lambda_2)k_1^2-(2\mu_2+\lambda_2)\rho_2\omega^2}.$$

By the first equation in Eq. (59), we have

$$\hat{u}_3(x_3)=\hat{u}_+\exp(\beta_1x_3)+\hat{u}_-\exp(-\beta_1x_3)$$

for some $\hat{u}_+,\hat{u}_-\in\mathbb{C}^3$. Then the last two equations in Eq. (59) implies

$$\begin{bmatrix}(\beta_1-\beta_2)\exp(\beta_1h_1) & (-\beta_1-\beta_2)\exp(-\beta_1h_1)\\ (\beta_1+\beta_2)\exp(\beta_1(h_1+h_2)) & (-\beta_1+\beta_2)\exp(-\beta_1(h_1+h_2))\end{bmatrix}\begin{bmatrix}\hat{u}_+\\ \hat{u}_-\end{bmatrix}=0. \tag{60}$$

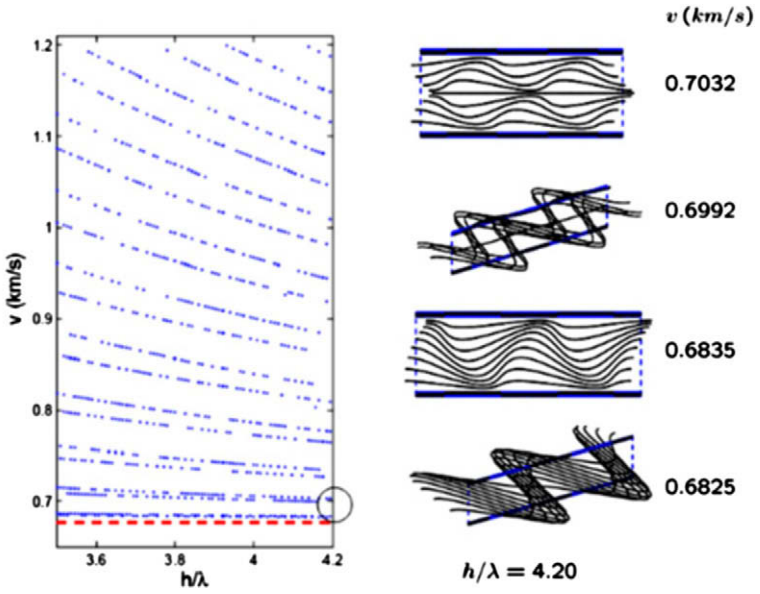

Fig. 7. The spectrum of the sandwich structure specified in Example 2.1 in the short wave length regime. Each "•" in the left figure denotes a point on the dispersion relations —— phase speed v vs h/λ. The phase speed of the transverse (shear) wave in the middle core is shown by the dashed line"– –" for comparison. The mode shapes of the lowest four branches are shown in the right figure. The numbers aside are their phase speeds.

Therefore, Eq. (59) admits a non-zero solution if and only if

$$(\beta_1+\beta_2)^2\exp(2\beta_1 h_2)-(\beta_1-\beta_2)^2=0. \tag{61}$$

We remark that the hypothesis $\hat{u}_1''=0$ on $[h_1,h_1+h_2]$, though seemingly *ad hoc*, is not groundless, as one can see from the first two mode shapes in Fig. 6 that the endpoints of lines in the middle layer remain nearly in a straight line. This additional hypothesis distinguishes the present model from that of Sorokin (2004). It is worthwhile noticing that the effects of the transverse shear of the middle layer and the in-plane motions of the top/middle layers could be included in this treatment. The resulting dispersion equation, however, losses its simplicity, see e.g. Nilsson (1990) for details in this direction. Further, based on the symmetry of the present sandwich structure we could proceed further to decouple the so-called "in-phase" waves and "anti-phase" waves, see Sorokin (2004) for the relevant calculations. Here we solve for the lowest dispersion relation determined by Eq. (61) numerically without decoupling them. In general only one of these two types of waves has lowest frequency for the same wavenumber k_1.

The lowest dispersion relation determined by Eq. (61) is shown in Fig. 6 in "□" markers. One can see that it agrees well with the exact result throughout the (h/λ)-interval under consideration. The reader is however cautioned that the good agreement between the present model and the exact result in the short wavelength regime, say, beyond the inflection point $h/\lambda\approx 1.8$, could be just a coincidence since the last two mode shapes in Fig. 6 are inconsistent with the hypothesis $u_1''\neq 0$ or $u_2=0$.

We remark that Eq. (61) in fact have infinitely many branches of solutions $\omega(k_1)$. For branches other than the lowest one, we have observed that they occasionally agree well with certain branches of the exact results. However, it is not clear why they agree. So these branches are not shown here.

4.3. Internal modes

In the regime where the wave length λ is a few times smaller than h, from the last two mode shapes in Fig. 6, we see that the displacements of the top/bottom layer are very small compared with those of the middle layer. Second, different branches of the dispersion relations are close to each other, see Fig. 2. In this case, the nearby branches are also important in determining the dynamic behavior of the sandwich structures. Therefore, a high-resolution numerical study based on the transfer matrix method (cf., Section 2) are performed for (h/λ)-interval [3.5,4.2] with its results shown in Fig. 7. Note that in the left of Fig. 7, the dispersion relations are displayed in terms of phase speeds v versus h/λ. For comparison, we show the phase speed of the bulk shear wave of the middle layer by the red dashed line "– –" in the bottom. The "•" markers show the results of the transfer matrix method. Corresponding to the lowest four branches (see circled area in the left figure of Fig. 7), the mode shapes at $h/\lambda=4.20$ are shown in the right of Fig. 7. The numbers along the mode shapes are the phase speeds of these modes.

From the mode shapes in Fig. 7, we see that the lowest four modes arise mainly from shear motions of the middle compliant layer. Compared with the phase speed of the bulk shear waves ($v_T=\sqrt{\mu_2/\rho_2}=0.6768$ km/s), the relative difference of these modes in phase speed is less than 3%. Therefore, finding the dispersion relations for these branches seems not to be a physically meaningful practice. The phase speeds decrease as the wavelength decreases. From the tendency shown by Fig. 7, we see that the gaps between various branches of dispersion relations would be smaller if the wavelength further decreases. We do not pursue simplified models here to explain these features of the dispersion relations.

5. Summary and discussion

We have considered a sandwich structure of two thin stiff layer and one thick compliant core. The method of transfer matrix is used to compute the full spectrum of the sandwich structure. The Hamiltonian formalism of the governing wave equations enables us to single out the relevant block in the transfer matrix and find all the initial points of the dispersion relations $\omega_\alpha(\mathbf{k})|_{\mathbf{k}=0}$. Based on the transfer matrix method, a systematic perturbation approach is demonstrated capable of finding higher order correction terms of the dispersion relations in the long wavelength limit. Finally, we find three simplified models that can predict the lowest branch of the dispersion relations in various regimes.

Much of the analysis in this paper can be applied to multi-laminated structures as well as to the sandwich structure. For additional layers, we simply include the local transfer matrix associated with the additional layers in the global transfer matrix (20). Therefore, the analysis in Section 3 is valid for multi-laminated structures as well. For the models in Section 4, the reader is however cautioned that the criteria for the applicable regimes of various models could be significantly different from the criteria for the particular sandwich structure in Example 2.1.

Further, the formalisms we have taken can be easily generalized to address laminated structures of anisotropic materials. The transfer matrix method presented in Section 2 is clearly valid for anisotropic materials. The only difference from isotropic materials is that the matrices $\mathbf{T}_i, \mathbf{Q}_i, \mathbf{R}_i$ defined in Eq. (5), and so the Hamiltonian matrix $\mathbf{H}_i$ in Eq. (10) may be more complicated and depend on the in-plane wavevector $\mathbf{k}$. The results in Section 3.1 are valid for general materials up to Eq. (33). In particular, if the materials are orthotropic, the matrices $\mathbf{T}_i$ remain diagonal, and so a formula like Eq. (34) can be obtained similarly. The perturbation method in Section 3.2 is also applicable to anisotropic materials, though the algebra is likely to be more formidable. For results in Section 4, generalizations to anisotropic materials may be difficult.

Acknowledgements

This work was carried out while Liping Liu held a position at the California Institute of Technology. The authors gratefully acknowledge the financial support of the US Office of Naval Research through the MURI Grant N00014-06-1-0730.

References

Atkinson, F.V., 1964. Discrete and Continuous Boundary Problems. Academic Press, New York.
Backström, D., Nilsson, A., 2006. Modeling flexural vibration of a sandwich beam using modified fourth-order theory. J. Sandwich Struct. Mater. 8, 465–476.
Backström, D., Nilsson, A., 2007. Modeling the vibration of a sandwich beams using frequency-dependent parameters. J. Sound Vibr. 300, 589–611.
Bonfiglioa, P., Pompolia, F., Peplowb, A.T., Nilssonb, A.C., 2007. Aspects of computational vibration transmission for sandwich panels. J. Sound Vibr. 303, 780–797.
Castaings, L., Hosten, B., 1994. Delta operator technique to improve the Thomoson–Haskell method stability for propagation in multilayered anisotropic absorbing plates. J. Acoust. Soc. Am. 95, 1931–1941.
Christensen, R.M., 1979. Mechanics of Composite Materials. Academic Press, New York.
Coddington, E.A., Levinson, N., 1955. The Theory of Ordinary Differential Equations. McGraw-Hill, New York.
Frostig, Y., Baruch, M., 1994. Free vibrations of sandwich beams with a transversely flexible core: a high order approach. J. Sound Vibr. 176, 195–208.
Haskell, N.A., 1953. The dispersion of surface waves on multilayered media. Bull. Seism. Soc. Am. 43, 17–34.
Kato, T., 1966. Perturbation Theory for Linear Operators. Springer, New York.
Knopoff, L., 1964. A matrix method for elastic wave problems. Bull. Seism. Soc. Am. 54, 431–438.
Lamb, H., 1917. On waves in an elastic plate. Proc. Roy. Soc. A 93, 114.
Lancaster, P., Rodman, L., 1995. Algebraic Riccati Equations. Oxford University Press, Oxford.
Landau, L.D., Lifshitz, E.M., 1986. Theory of Elasticity. Pergamon Press, New York.
Lo, K.H., Christensen, R.M., Wu, E.M., 1977a. A high-order theory of plate deformation. Part 1: Homogeneous plates. J. Appl. Mech. 44, 663–668.
Lo, K.H., Christensen, R.M., Wu, E.M., 1977b. A high-order theory of plate deformation. Part 2: Laminated plates. Trans. ASME, Ser. E: J. Appl. Mech. 44, 669–676.
Mead, D.J., Markus, S., 1969. The forced vibration of a three-layer, damped sandwich beam with arbitrary boundary conditions. J. Sound Vibr. 10, 163–175.
Mindlin, R.D., 1951. Influence of rotatory inertia and shear on flexural motions of isotropic, elastic plates. J. Appl. Mech. 18, 31–38.
Mindlin, R.D., 1960. In structural mechanics. In: Goodier, J.N., Hoff, N.J. (Eds.), Waves and Vibrations in Isotropic, Elastic Plates. Pergamon Press, New York, pp. 199–232.
Moler, C., Loan, C.V., 2003. Ninteen dubious ways to compute the exponential of a matrix, twenty-five years later. SIAM Rev. 45, 3–49.
Nayfeh, A.H., 1995. Wave Propagation in Layered Anisotropic Media: With Applications to Composites. Elsevier, Amsterdam.
Nilsson, A.C., 1990. Wave propagation in and sound transmission through sandwich plates. J. Sound Vibr. 138, 73–94.
Nosier, A., Kapania, R.K., Reddy, J.N., 1993. Free vibration analysis of laminated plates using a layer-wise theory. AIAA J. 31, 2335–2346.
Reissner, E., 1945. The effect of transverse shear deformation on the bending of elastic plates. J. Appl. Mech. 12, A69–A77.
Reissner, E., 1947. On the bending of elastic plates. Quart. Appl. Math. 5, 55–68.
Sorokin, S.V., 2004. Analysis of wave propagation in sandwich plates with and without heavy fluid loading. J. Sound Vibr. 271, 1039–1062.
Sorokin, S.V., 2006. Analysis of propagation of waves of purely shear deformation in a sandwich plate. J. Sound Vibr. 291, 1208–1220.
Stephen, N.G., 1997. Mindlin plate theory: best shear coefficient and higher spectra validity. J. Sound Vibr. 202, 539–553.
Thomsen, O.T., Bozhevolnaya, E., Lyckegaard, A. (Eds.), 2005. Sandwich Structures 7: Advancing Sandwich Structures and Materials: Proceedings of the 7th International Conference on Sandwich Structures. Springer, Berlin.
Timoshenko, S., 1921. On the correction for shear of the differential equation for transverse vibrations of prismatic bars. Philos. Mag. Ser. 6 (41), 744–746.
Timoshenko, S., 1922. On the transverse vibrations of prismatic bars. Philos. Mag. Ser. 6 (43), 125–131.
Timoshenko, S., 1940. Strength of Materials. Van Nostrand, New York.
Timoshenko, S., Woinowsky-Krieger, S., 1959. Theory of Plates and Shells. McGraw-Hill, New York.
Ting, T.C.T., 1996. Anisotropic Elasticity: Theory and Applications. Oxford University Press, Oxford.
Yang, M.J., Qiao, P.Z., 2005. Higher-order impact modeling of sandwich structures with flexible core. Int. J. Solids Struct. 42, 5460–5490.
Zettl, A., 2005. Sturm-Liouville Theory. AMS, Providence.